Nuclear Propulsion through Direct Conversion of Fusion Energy:

The Fusion Driven Rocket

Phase I Final Report

John Slough, Anthony Pancotti, David Kirtley, Christopher Pihl, Michael Pfaff

MSNW LLC
8551 154th Ave NE
Redmond WA. 98052
425-867-8900

NASA Grant: NNX12AR39G
September 30, 2012

Summary

The Fusion Driven Rocket:

Nuclear Propulsion through Direct Conversion of Fusion Energy

The future of manned space exploration and development of space depends critically on the creation of a dramatically more proficient propulsion architecture for in-space transportation. A very persuasive reason for investigating the applicability of nuclear power in rockets is the vast energy density gain of nuclear fuel when compared to chemical combustion energy. Current nuclear fusion efforts have focused on the generation of electric grid power and are wholly inappropriate for space transportation as the application of a reactor based fusion-electric system creates a colossal mass and heat rejection problem for space application. The Fusion Driven rocket (FDR) represents a revolutionary approach to fusion propulsion where the power source releases its energy directly into the propellant, not requiring conversion to electricity. It employs a solid lithium propellant that requires no significant tankage mass. The propellant is rapidly heated and accelerated to high exhaust velocity (> 30 km/s), while having no significant physical interaction with the spacecraft thereby avoiding damage to the rocket and limiting both the thermal heat load and radiator mass. In addition, it is believed that the FDR can be realized with little extrapolation from currently existing technology, at high specific power (~ 1 kW/kg), at a reasonable mass scale (<100 mt), and therefore cost. If realized, it would not only enable manned interplanetary space travel, it would allow it to become common place.

The key to achieving all this stems from research at MSNW on the magnetically driven implosion of metal foils onto a magnetized plasma target to obtain fusion conditions. A logical extension of this work leads to a method that utilizes these metal shells (or liners) to not only achieve fusion conditions, but to serve as the propellant as well. Several low-mass, magnetically-driven metal liners are inductively driven to converge radially and axially and form a thick blanket surrounding the target plasmoid and compress the plasmoid to fusion conditions. Virtually all of the radiant, neutron and particle energy from the plasma is absorbed by the encapsulating, metal blanket thereby isolating the spacecraft from the fusion process and eliminating the need for large radiator mass. This energy, in addition to the intense Ohmic heating at peak magnetic field compression, is adequate to vaporize and ionize the metal blanket. The expansion of this hot, ionized metal propellant through a magnetically insulated nozzle produces high thrust at the optimal Isp. The energy from the fusion process, is thus utilized at very high efficiency.

During phase I the metal foil convergence and compression physics has been analyzed analytically as well as modeled in 3D with the ANSYS Multiphysics® code. These results were used to extend modeling to the ongoing 2D resistive Magnetohydrodynamic analysis of the fusion plasma compression. The initial determination of the optimum compression methodology, materials, and fuels to achieve required fusion power and specific mass for various missions has been performed, and a systems-level model along with the initial propulsion system design has been carried out and is presented as well.

A range of both manned and unmanned missions was considered for which this fusion propulsion system would be enabling or critical. Manned mission architecture to Mars similar to the NASA Design Reference Mission (DRM) 3.0 was considered as part of a mission analysis for two mission designs - a 90 and 30 day trip to/from Mars with a discussion of the results for various fusion gains for the FDR.

Expanding on these results from the phase I, the phase II effort will focus on achieving three key criteria for the Fusion Driven Rocket to move forward for technological development: (1) the physics of the FDR must be fully understood and validated, (2) the design and technology development for the FDR required for its implementation in space must be fully characterized, and (3) an in-depth analysis of the rocket design and spacecraft integration as well as mission architectures enabled by the FDR need to be performed. Fulfilling these three elements form the major tasks to be completed in the Phase II study. A subscale, laboratory liner compression test facility will be assembled with sufficient liner kinetic energy (~ 0.5 MJ) to reach fusion gain conditions. Initial studies of liner convergence will be followed by validation tests of liner compression of a magnetized plasma to fusion conditions. A complete characterization of both the FDR and spacecraft will be performed and will include conceptual descriptions, drawings, costing and TRL assessment of all subsystems. The Mission Design Architecture analysis will examine a wide range of mission architectures and destination for which this fusion propulsion system would be enabling or critical.

Table of Contents

2. Introduction

The future of manned space exploration and development of space depends critically on the creation of a dramatically more proficient propulsion system for in-space transportation. This has been recognized for many years. A very persuasive reason for investigating the applicability of nuclear power in rockets is the vast energy density gain of nuclear fuel when compared to chemical combustion energy. The combustion of hydrogen and oxygen has an energy release of 13 MJ/kg, whereas the fission of ^{235}U yields approximately 8×10^7 MJ/kg and the fusion of deuterium and tritium has a 3.6×10^8 MJ/kg yield. So far, the use of fission energy represents the nearest term application of nuclear power for propulsion. Several fission based propulsion schemes have been proposed for in-space transportation, including pulsed nuclear explosions and the Nuclear Thermal Rocket (NTR).[1]

In the NTR a cooling fluid or propellant is passed through a core of material that has been heated by fission. This makes the NTR effectively a heated gas rocket. With the present limitations of materials, NTR gas temperatures cannot exceed chemical propulsion gas temperatures. The use of hydrogen provides for an increase in Isp to 900 s. With $\Delta v \sim 9$ km/sec the propellant mass is reduced by an order of magnitude for a given spacecraft mass. Unfortunately, this is considerably offset by increased spacecraft mass (payload, structure, shielding, tankage etc.). A significant mass is required for the low mass density propellant (H_2) as the specific gravity of liquid hydrogen is around 0.07, compared to 0.95 for an O_2-H_2 chemical engine. The net result then is a propulsion system that is better than chemical, but not enough to really be a "game changer". Proposed Nuclear Electric (NE) systems employ high Isp thrusters like the ion and Hall thrusters which solves the propellant Isp issue. The problem for NE is the inherent inefficiency of the generation of electrical power. Shedding the excess reactor heat requires an enormous radiator mass. The large reactor and power conversion masses just add to this problem making for too low a specific power (ratio of jet power to system mass) for rapid space transport.

Invoking nuclear fusion for space propulsion, at least as it has been envisioned up till now, does not significantly change this picture as it has been developed primarily as an alternate source for electrical grid power. This endeavor is far from completion, and even if nuclear fusion were to be eventually developed for terrestrial power generation, the resulting power plant would be extremely unlikely to have any role in space propulsion for all the same reasons that trouble NE - but worse.

If one were to imagine the optimal solution out of the this quandary, it would be a propulsion system where

(1) the power source releases its energy directly into the propellant, not requiring conversion to electricity

(2) the propellant requires no significant tankage mass by being a solid, and where

(3) the propellant is rapidly heated and accelerated to high exhaust velocity (> 20 km/s), while

(4) there is no significant physical interaction with the spacecraft thereby limiting thermal heat load, spacecraft damage, and radiator mass.

In addition, if these four elements could be accomplished:

(5) with little extrapolation from currently existing technology,
(6) at high specific power (~ 1 kW/kg) and
(7) at reasonable scale (<100 mt), power (multi MW) and cost (< 1$B),

it would not only enable manned interplanetary space travel, it would allow it to become common place. The Fusion Driven Rocket (FDR), to be further elucidated in this proposal, possesses all seven of these attributes. If the FDR lives up to its potential, it would represent the most significant and revolutionary mode of space transport yet devised by man. For this to be a reality, several criteria must be met:

(1) the physics of the FDR must be fully understood and validated,
(2) the design and technology development for the FDR required for its implementation in space must be fully characterized, and
(3) an in-depth analysis of the rocket design and spacecraft integration as well as mission architectures enabled by the FDR need to be performed.

The phase I effort initiated under the NIAC program has focused on these three elements. The results from these efforts form the basis of this final report. This report contains a description of the Fusion Driven Rocket concept and describes the advantages of the Inductively Driven Liner Compression (IDLC). A brief introduction of several other fusion concepts is given as a base of comparison and to fully illustrate key concept such as proper energy scaling and isolation or standoff.

2.1. A New Approach to Fusion Propulsion: The Fusion Driven Rocket

This is certainly not the first time that fusion energy has been proposed as the ultimate solution for rapid manned space travel. Past efforts in this regard have all come to be dismissed, and rightfully so, primarily for the following two reasons. The first has been alluded to already. The propulsion system is reactor based. The straightforward application of a reactor-based fusion-electric system creates a colossal mass and heat rejection problem for space application. In a detailed analysis for the most compact tokamak concept, the spherical torus, spacecraft masses of 4000 mt were projected.[2] The maximum launch mass would need to be less than 200 mt if current chemical rockets are used for launch to LEO.

Virtually all previous fusion propulsion systems needed to employ alternate fusion reactions that produce primarily charge particles as fusion products to avoid the large energy loss from fusion neutrons. The most tenable were D-^{3}He $\Rightarrow$ P(14.7 MeV) + ^{4}He(3.6 MeV) and P-^{11}B $\Rightarrow$ 3 ^{4}He(2.9 MeV). These reactions require much higher plasma temperatures and are orders of magnitude more difficult to achieve than the D-T $\Rightarrow$ n(14.1 MeV) + ^{4}He(3.5 MeV) which is the most readily achieved reaction and the only one seriously considered for earth based fusion reactors. With the much lower fusion gain for these advanced fuels, the recirculating power needed to produce the fusion reaction becomes enormous dooming it to being no better than the fission reactor based alternatives.

What is required is a completely different approach to what has been considered in the past if one is to make practical use of fusion energy for space propulsion. It is illustrative to examine what makes chemical propulsion so attractive. A principle reason is the fact that the power delivered through chemical combustion can be made as large or as small as needed; from the Atlas heavy rocket at 13 GW, to the conventional automobile (130 kW). It is worth noting that at

lower power, the combustion is pulsed to achieve the greater efficiency obtained at high temperature without incurring the massive cooling requirements and thermal damage that would result from continuous operation at small scale.

As first demonstrated at Trinity site (fission) and then at Enewetak Atoll (fusion), the ignition of nuclear fuels have certainly confirmed the ability to produce copious energy yields from nuclear energy, dwarfing that of the Atlas V by many orders of magnitude. The challenge is how to have the release of nuclear energy occur in such a manner as to be a suitable match to that desired for manned spaceflight missions: multi-megawatt jet power, low specific mass α (~ 1 kg/kW) at high Isp (> 2,000 s). It would appear that for at least nuclear fission, there is no real possibility of scaling down to an appropriately low yield as a certain critical mass (scale) is required to achieve the supercritical chain reaction needed for high energy gain. Fission nuclear pulse propulsion then, such as that envisioned in the Orion project, ends up with a thrust in the millions of mt which would only be suitable for spacecraft on the order of 10^7 mt - the mass of over 100 aircraft carriers!

Fortunately, the critical mass/scale for fusion ignition can be much smaller. The criteria to achieve D-T fusion ignition, at a nominal fuel (plasma) temperature of 10 keV, is the attainment of a density-radius product of $\rho \cdot R \sim 0.1$ g/cm^2. This can be accomplished with a three dimensional compression of a spherical cryogenic fuel pellet of millimeter scale. Here it is assumed that the inertia of the small pellet is sufficient to confine the plasma long enough for the burn to propagate through the pellet and thereby produce an energy gain G ~ 200 or more (G = fusion energy/initial plasma energy). This Inertial Confinement Fusion (ICF) approach has been actively pursued by the National Nuclear Security Administration (NNSA) of the DOE for decades as it represents essentially a nano-scale version of a fusion explosive device. Because of the small scale and tiny masses, the energy delivery system required to heat the pellet to fusion temperature must be capable of doing so on the nanosecond timescale. It appears that the most promising solution to accomplish this is with a large array of high power pulsed lasers focused down on to the D-T pellet. The actual target compression is obtained by ablating the surface of a shell surrounding the fuel. This creates a strong inward compression of the pellet from the remaining outer shell due to momentum conservation. This compression, if strong enough, brings the fuel to the temperature and density required for fusion burn as indicated in Fig. 1.

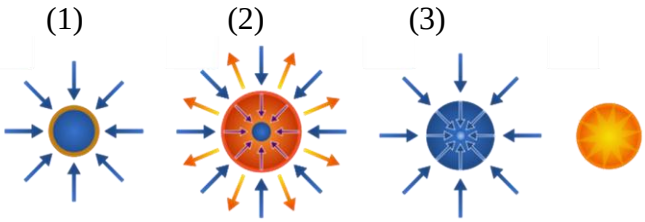

Figure 1: (1) x-rays, laser, or ion energy deposition rapidly heats shell (liner) surrounding D-T fuel. (2) fuel is compressed by the rocket-like blow-off of the ablated material. (3) fuel core reaches density and temperature for fusion ignition yielding ~ 200 times the compressional energy.

The National Ignition Facility (NIF) at Livermore National Laboratory is now in the process of testing a laser driven pellet implosion capable producing significant fusion gain for the first time. This will be a very significant milestone for the generation of fusion energy at small scale. While the expected energy yield is in the range appropriate for propulsion (E ~ 20-100 MJ), the scale and mass of the driver (lasers and power supplies) is not, as it requires an aerial photograph to image the full system. It would seem one is back in the same quandary as before. However there

have been three breakthrough realizations in the last several years that have provided the keys to achieving inertial fusion at the right scale in an efficient and appropriate manner for space propulsion. They primarily concern the enhanced confinement provided by significant magnetization of the target plasma which considerably eases the compressive requirements to achieve fusion gain and even fusion ignition. This new approach to fusion is aptly referred to as Magneto-Inertial Fusion, and will now be briefly described.

2.1.1 Magneto Inertial Fusion (MIF)

The notion of using other means than an array of high power lasers to compress the target to fusion conditions goes back as far as the nineteen fifties. Heavy ions and metal shells (liners) were two of the most promising. They all had in common the basic approach of ICF shown in Fig. 1**Error! Reference source not found.**: the outer shell or liner is driven directly or indirectly inward compressing the inner target to fusion conditions. Regardless of method, this compression must uniform, intense and accomplished with great precision resulting in large, high voltage and expensive driver systems. By the mid-nineties it was realized that the presence of a large magnetic field in the target would substantially suppress the thermal transport, and thus lower the imploding power needed to compress the target to fusion conditions. With more time before the target plasma thermal energy was dissipated, a much more massive confining shell could be employed for direct compression, with the dwell time of the confining (metal) shell now providing for a much longer fusion burn time. The liner did not need to be propelled inward by ablation but could be driven by explosives or even magnetic fields. In a seminal paper by Drake et al.[3] it was shown that if the imploding shell on to the magnetized target were fully three dimensional, fusion gain could be achieved on a small scale with sub-megajoule liner (shell) kinetic energy. There was no known way to accomplish this at that time, but it was feasible at least in theory. The second major theoretical result was obtained by Basko et al.[4] who showed that for a sufficiently magnetized target plasma, fusion ignition would occur even when the restrictive condition that $\rho \cdot R > 0.1$ g/cm^2 was far from being met. Ignition was now possible as long as the magnetic field-radius product, $B \cdot R >$ 60 T-cm. Thus fusion ignition could be obtained for MIF targets with much lower compression than required for ICF as Figure **2** indicates. The final critical element to enable fusion energy to be utilized for space propulsion was a practical method to directly channel the fusion energy into thrust at the appropriate Isp. It is believed that such a method has been determined at MSNW that is supported by both theory and experiment. A description of the operating principles of the Fusion Driven Rocket will now be given.

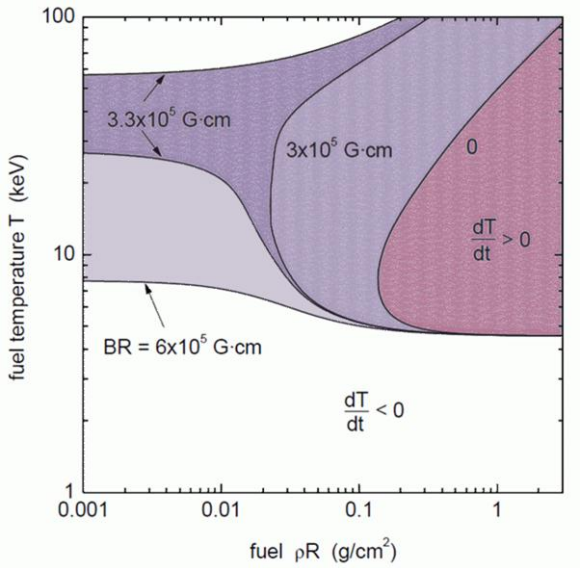

Figure 2: The BR form of the Lindl-Widner (L-W) diagram. Ignition curves for different product BR (taken from Ref. 4). When the BR parameter exceeds the threshold value, the dT/dt > 0 region extends to infinitely small ρR and ignition

2.1.2 Inductively-Driven Foil Compression (IDFC) of a Magnetized Plasmoid

It was clear that fusion ignition conditions could be achieved at small scale by applying the kinetic energy of a significantly more massive metal shell to compress the target plasma to high density and temperature. What remained to be solved were the following four challenges:

(1) how to do this without invoking a massive and complex driver,

(2) how to do it in a manner that is efficient and capable of repetitive operation,

(3) how to create a suitable magnetized plasma target, and

(4) how to transfer the fusion energy into a suitably directed propellant.

The key to answering all four "hows" stems from current research being done at MSNW on the magnetically driven 3D implosion of metal foils on to an FRC target for obtaining fusion conditions. A logical extension of this work leads to a method that utilizes these metal shells to not only achieve fusion conditions, but then to become the propellant as well. The basic scheme for FDR is illustrated and described in Fig. 3. The two most critical issues in meeting challenges (1) and (2) for MIF, and all ICF concepts for that matter, is driver efficiency and "stand-off" – the ability to isolate and protect fusion and thruster from the resultant fusion energy. By employing metal shells for compression, it is possible to produce the desired convergent motion inductively by inserting the metal sheets along the inner surface of cylindrical or conically tapered coils. Both stand-off and energy efficiency issues are solved by this

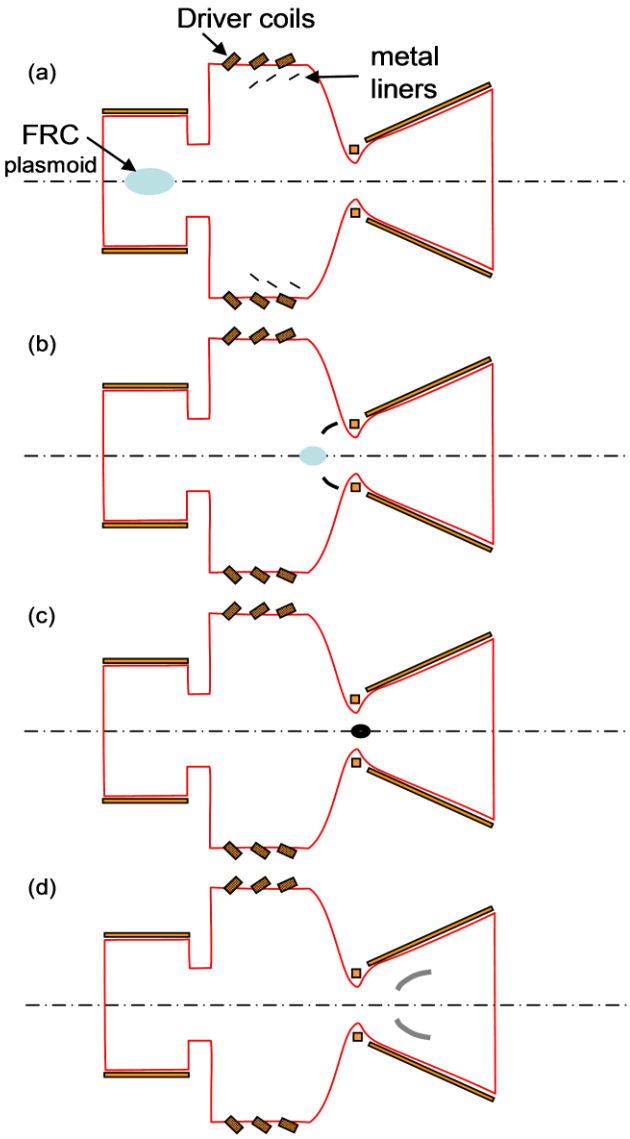

Figure 3: Schematic of the inductively driven metal propellant compression of an FRC plasmoid for propulsion. (a) Thin hoops of metal are driven at the proper angle and speed for convergence onto target plasmoid at thruster throat. Target FRC plasmoid is created and injected into thruster chamber.
(b) Target FRC is confined by axial magnetic field from shell driver coils as it translates through chamber eventually stagnating at the thruster throat.
(c) Converging shell segments form fusion blanket compressing target FRC plasmoid to fusion conditions.
(d) Vaporized and ionized by fusion neutrons and alphas, the plasma blanket expands against the divergent magnetic field resulting in the direct generation of electricity from and the back EMF and a directed flow of the metal plasma out of the magnetic nozzle.

arrangement. The metal shell can be positioned a meter or more from the target implosion site with the coil driver both physically and electrically isolated from the shell. The driver efficiency can be quite high as the coil driver is typically the inductive element of a simple oscillating circuit where resistive circuit losses are a small fraction of the energy transferred. With an in-line element as rudimentary as a diode array, any magnetic energy not imparted to the liner can be recovered back into the charging system after the shell is driven off with the first half cycle. The feasibility of rapidly accelerating inward and compressing thin hoops of aluminum and copper in this manner was first demonstrated by Cnare[5]. Since then, the technique has been employed in several experiments to obtain very high magnetic fields as it will be done here. Even though there is essentially no magnetic field within the hoops initially, there is enough flux leakage during the inward acceleration that at peak compression the axial magnetic field that is trapped inside the now greatly thickened wall can reach as high as 600 T.[6] As will be seen this field is considerably higher than required for compression of the FRC to have ignition and substantial fusion gain.

The next challenge to be considered is the magnetized plasma to be used as the fusion target. Spaced-based fusion demands a much lower system mass. The lowest mass system by which fusion can be achieved, and the one to be employed here, is based on the very compact, high energy density regime of magnetized fusion employing a compact toroidal plasmoid commonly referred to as a Field Reversed Configuration (FRC).[7] It is of paramount advantage to employ a closed field line plasma that has intrinsically high β (plasma/magnetic pressure ratio), and that can be readily translated and compressed, for the primary target plasma for MIF. Of all fusion reactor embodiments, only the FRC plasmoid has the linear geometry, and sufficient closed field confinement required for MIF fusion at high energy density. Most importantly, the FRC has already demonstrated both translatability over large distances[8] as well as the confinement scaling with size and density required to assure sufficient lifetime to survive the compression timescale required for liner-based inertial fusion. FRCs have also been formed with enough internal flux to easily satisfy the B·R ignition criteria at peak compression.

At a nominal liner converging speed of 3 km/s, a 0.2 m radius FRC typical of operation on the LSX FRC device would be fully compressed in 67 μs which is only a fraction of the lifetime that was observed for these FRCs (~ 1 ms).[9] The target plasma to be employed in FDR will thus be an FRC plasmoid.

Finally, to complete the fourth challenge, a straightforward way to convert the fusion energy into propulsive energy must be devised. It is in this regard that the approach outlined here is uniquely capable. It starts by employing an inductively driven thin metal liner first to compress the magnetized plasma. As the radial and axial compression proceeds, this liner coalesces to form a thick ($r > 5$ cm) shell that acts as a fusion blanket that absorbs virtually all the fusion energy as well as the radiated plasma energy during the brief fusion burn time. This superheated blanket material is subsequently ionized and now rapidly expands inside the divergent magnetic field of the nozzle that converts this blanket plasma energy into propulsive thrust. It would be possible to also derive the electrical energy required for the driver system from the back EMF experienced by the conical magnetic field coil circuit via flux compression.[10] It was found however that the power required for recharging the energy storage modules for the metal liner driver coils could readily be obtained from conventional solar electric power (SEP). As will be discussed, for very rapid, high power missions, the flux compressor/generator option could be

developed. For the near term manned mars missions the SEP requires the least technology development, lowest cost and highest TRL level.

In the following sections of this report, the phase I effort is summarized and presented for three major areas of research: The physics of the fusion reaction, the optimized mission design for a fusion rocket, and an initial description of the spacecraft system design.

3. Phase I Technical Objectives Aachieved

The primary goal of this phase I effort was be to bring The Fusion Driven Rocket from TRL 1 (Basic principles observed and reported) to TRL 2 (Technology concept and application formulated). The research was organized into 3 major three tasks, each iterating on the other tasks in order to generate a roadmap to further develop the concept in Phase II and beyond. The final FDR road map is discussed in Section 4. Each of the three tasks of phase I have been further broken down into individual subtasks. The tasks and related subtasks are listed below and are then discussed in detail in Sections 3.1 through 3.3.

Task 1 – Fusion Physics and Formation Technologies

(a) Investigate physic of IDFC fusion for purposes of propulsion
(b) Determine optimum compression geometries, materials, and fuels to achieve required fusion power, specific mass and optimum Isp
(c) Design of validation experiment require in Phase II

Task 2 – Mission definition and Trade analysis

(a) Examine the missions for which FDR is most enabling or critical
(b) Down select mission options and develop coherent mission architecture
(c) Preform trade-study analysis based on fusion parameters to optimize mission design

Task 3 – Spacecraft system design

(a) Based on the chosen mission type determine required payload mass, system scale, and geometry
(b) Establish preliminary estimates vehicle weight including requirements for propellant and energy storage, thermal radiators, and fusion product shielding

An optimal method for achieving the compressional heating required to reach fusion gain conditions based on the compression of a Field Reversed Configuration plasmoid (FRC) was ascertained during Phase I. This research determined that an inductive technique could be employed to accelerate an array of thin, lithium metal bands radially inward to create a three dimensional compression of the target FRC. It was also conceived that the FRC can be formed inside the main reaction chamber using a rotating magnetic field (RMF) generated by antennas located outside the reactor vessel or by injection through end ports. No ports or opening of the reactor is required during fusion burn with RMF. The metal bands can be located a meter or more from the target implosion site, and with inductive drive the driver coils are physically positioned outside the reactor vacuum wall. An effective fusion blanket is formed with the convergence of the bands absorbing the fusion energy as well as the radiated plasma energy during the brief fusion burn. The resultant vaporized and ionized blanket shell expands compressing the external magnetic field providing for direct energy conversion. Several aspects of the process have been explored experimentally and numerically and are present in this final Report. A description of a sub-megajoule experiment that was designed as a result of this

research has been proposed as a validation experiment to be conducted under Phase II. Further description experimental setups as well as the explanation of the governing physic scaling laws are presented in Section 3.1.

To evaluate the potential of a fusion propulsion system, it was important to understand which missions are best suit for its application. Because of the high level of energy storage of fusion material, FDR is most beneficial for mission that are impossible or impractical with chemical systems, where the mass of propellant became too large do to exponential scaling of the rocket equation. Ultimately, a propulsion system like FDR, with high Isp, is needed for mission beyond near Earth. FDR would certainly have an application for Jupiter, or its icy moons, Neptune, asteroid rendezvous, and numerous other high ΔV interplanetary missions. For this Phase I analysis an in-depth analyses of a Mars mission was chosen as this would most likely be the mission for first application of the FDR. In addition, there exists a large body of reference work for propulsion systems to Mars. It is technically feasible to accomplish Mars transit with a variety of propulsion system, and therefore it has become a kind of interplanetary propulsion benchmark. By investigated a manned mission to Mars it was possible to directly compare with other techniques. As will be shown, the FDR allows for a much faster trip time, reducing the physical demands on astronauts and minimizing the reduction in bone and muscle loss as well as radiation exposure. FDR also has the advantage of higher payload mass fraction delivered to Mars. This means for a desired payload required for Mars exploration only a fraction of material compared to chemical propulsion system has to be launched off the earth's surface (which is a major cost and deterrent for Mars missions). The full mission analysis highlighting the tradeoffs between mission times, payload mass fraction, and expected fusion gains are explained in further detail in Section 3.2.

Because of the open parameter space of the mission design and large variation in potential fusion gains it was inappropriate to perform a full spacecraft system design as part of the year one effort. Instead it was decided that this task should be giving a higher priority under Phase II, and only a preliminary investigation of major components would be examined under Phase I. These major areas of spacecraft design focused on sub components such as solar panels, which were a major fact in mission design, which largely impacted overall spacecraft masses. The Major driving factor behind this investigate was to estimate the mass of material that would need to be launched to LEO and the number of launch vehicles required to do so. More discussion on the spacecraft system design can be found in Section 3.3.

3.1 Physics of Inductively Driven Liner Compression (IDLC)

The analysis of the liner implosion was carried out for both a subscale validation experiment that could be performed with existing equipment at MSNW and the Plasma Dynamics Laboratory at the University of Washington, as well as a full-scale reactor prototype.

For the purposes of the analysis given here, a very conservative liner kinetic energy, E_L = 560 kJ was assumed from the existing 1.4 MJ capacitor bank based on modeling and other inductive liner compression experiments.[11,12] The dynamics of the liner implosion are governed by the equation:

$$M_L \frac{d^2 r}{dt^2} = \left(\frac{B_{in}^2}{2\mu_0} - \frac{B_{ext}^2}{2\mu_0} \right) 2\pi r w \tag{1}$$

where M_L is the liner mass, and w the liner width. During the liner acceleration very little flux leaks through the liner ($B_{in} << B_{ext}$). On energizing the driver coil, due to the small gap and the inertia of a solid metal liner, the magnetic field rapidly increases and is then maintained at a roughly constant amplitude ($B_{ext} \sim$ const.) during the inward motion of the liner as the increasing flux from the driver circuit into the gap between the coil and liner is countered by the increasing gap cross-sectional area. This liner/magnetic behavior was confirmed by 3D modeling with the Maxwell® 3D electromagnetic code. With this approximation Eq. (1) is readily integrated. Given the liner mass $M_L = 2\pi r_L \cdot w \cdot \delta \cdot \rho_L$, where δ is the liner thickness and ρ_L the liner density, the liner velocity is:

$$v_L = \left(\frac{r(t)}{2\mu_0 r_L \delta \rho_L} \right) B_{ext}^2 t \quad = 125 \frac{\tau}{\delta} B_{ext}^2 \tag{2}$$

where τ is the period of acceleration at constant B_{ext}. An aluminum liner was assumed in evaluating the right hand side of Eq. (2). B_{ext}, is determined by the stored capacitor energy minus liner energy which is (1.4-0.56) MJ ~ 0.8 MJ for the PDL fast energy delivery system. Equating this to the magnetic energy stored in the annular of gap of the liners yields B_{ext} = 9 T when the liner has moved inward by 15% of the initial coil (liner) radius of 0.4 m. While the liner continues to be accelerated, the rate drops dramatically as the area between the coil and liner grows while the capacitor bank energy has been fully transferred to the coil. For the liner to have moved inward 6 cm in 40 μsec under a constant magnetic force implies a terminal velocity of v_L = 3 km/s, consistent with that predicted by the above equation for a 0.2 mm aluminum liner.

The key process of the dynamical behavior of the convergent aluminum foil liners was also analyzed with the ANSYS Multiphysics® code. Here the non-linear behavior of the aluminum liners was modeled based on the magnetic pressure profile in time and space similar to that predicted by Eq. (1) and Maxwell®. The result from a calculation with the physical setup similar to the subscale validation experiment is illustrated in Figure **4**.

As mentioned, the FRC has been selected as the target plasmoid. A schematic of FRC is

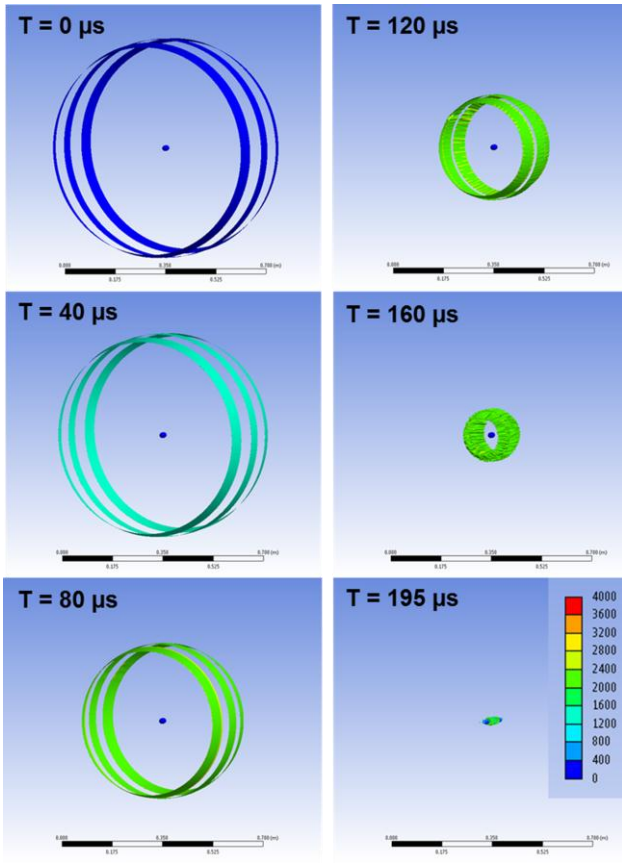

Figure 4: ANSYS Multiphysics® calculation of the 3D behavior of three 40 cm radius, 5 cm wide, 0.2 mm thick Aluminum liners converging onto a stationary test target. The scale of the ellipsoid target (1×3.5 cm) is that anticipated for an initially 20 cm radius FRC compressed to 1 megabar energy density. Color scale indicates liner velocity.

shown in Figure 5. The liner moves in radially compressing the FRC until it stagnates due to the

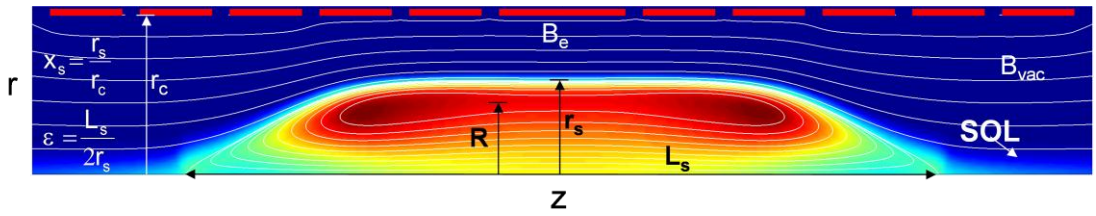

Figure 5: Elongated Field Reversed Configuration (FRC) Equilibrium Magnetic Field lines and Pressure Contours

rising pressure from the trapped magnetic field (and FRC plasma). The energy within the FRC separatrix at peak compression is dominated by plasma energy that must be in radial pressure balance with the edge axial magnetic field B_0, so that one can write:

$$E_L = \frac{1}{2} M_L v_L^2 = 3 n_0 k T_0 \cdot \frac{4}{3} \pi r_0^3 \varepsilon = \frac{B_0^2}{\mu_0} \pi r_0^3 \varepsilon \tag{3}$$

where the zero subscript indicates values at peak compression. The last expression in Eq. (3) reflects the reasonable assumption that $r_s \sim r_0$ and magnetic pressure balance ($2n_0kT_0 = B_0^2/2\mu_0$). One has then for the fusion energy produced in the FRC during the shell's dwell time τ_D at peak compression:

$$\begin{aligned} E_{fus} \cong & \quad 1.2 \times 10^{-12} n_0^2 \langle \sigma v \rangle \frac{4}{3} \pi r_0^3 \varepsilon \tau_D \\ = & \quad 1.1 \times 10^{-42} n_0^2 T_0^2 \frac{r_0^4}{v_L} \varepsilon \end{aligned} \tag{4}$$

where n_0 and T_0 are the peak density and temperature, and where the liner shell dwell time at peak compression, $\tau_D \sim 2r_0/v_L$. The dwell time can actually be much longer for a thick liner, but the more conservative dwell time is assumed here. Liner compressive effects are also ignored in this zero order analysis. The usual approximation for the D-T fusion cross section in this temperature range: $\langle \sigma v \rangle \cong 1.1 \times 10^{-31}\ T^2(\text{eV})$ was also assumed. Pressure balance, together with expressions (3) and (4) yields for the fusion gain:

$$\begin{aligned} G = \frac{E_{fus}}{E_L} = & \quad 1.73 \times 10^{-3} \sqrt{\frac{M_L}{l_0}} B_0 \\ = & \quad 4.3 \times 10^{-8} \sqrt{M_L}\ E_L^{11/8} \end{aligned} \tag{5}$$

where l_0 ($= 2r_0 \cdot \varepsilon$) is the length of the FRC at peak compression. The last expression is obtained from the adiabatic scaling laws for the FRC:[15]

$$E_L \sim B_0^2 r_0^2 l_0 \sim B_0^{4/5}$$
$$l_0 \sim r_0^{2/5} \sim B_0^{-1/5} \quad (6)$$

in order to express G in terms of the liner kinetic energy and mass, E_L and M_L only.

Starting with typical FRC parameters one obtains the final FRC parameters assuming both an adiabatic radial and axial compression from the 3D convergence of the liners. The ends of the merged liners are observed to do this naturally in the ANSYS® calculations (see

Figure 4), as the end liners have a significant axial velocity component and are unimpeded by the FRC presence as it contracts axially inward. The unique behavior of the FRC equilibrium to axial liner compression is quite valuable in this context as it provides for magnetic insulation of the FRC boundary regardless of the increase in the ratio of plasma to magnetic energy that comes with the increased axial compression. The proper plasma parameters for the initial FRC are found by extrapolation back from the desired final state. The compression that is applied by the liners is adiabatic with regard to FRC as the liner motion is far less than the plasma sound speed. The key adiabatic relations for the FRC are stated in

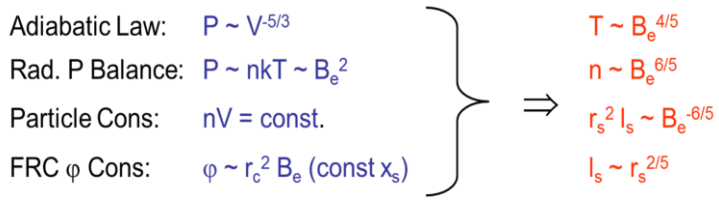

Figure 6: FRC adiabatic scaling laws used to obtain initial FRC conditions from the desired conditions at full compression.

Figure 6.

Injecting the FRC into the liners is delayed to until the liners have been fully accelerated and have moved inward away from the driver coils. For the validation experiment this would be accomplished by injecting two FRCs and merging them inside the liner as this permits an axially stationary liner compression which considerably eases the diagnostic evaluation of the compression process as the target remains fixed. Adding a translating component to the liner motion would be something to be addressed for the space propulsion application after success with the validation experiment.

3.1.1. IDLC validation

As mentioned the scale of the validation experiments is based on the generation of an FRC similar to that produced in the LSX FRC experiments.[13] Using the FRC adiabatic scaling laws listed in Figure 6, and assuming E_L = 560 kJ, the convergence of a set of three aluminum liner set with an initial total mass of 0.18 kg would produce a peak

Parameter	Merged FRC ($t = \tau_{1/4}$)	Radial FRC Compression	Axial FRC Compression
v_L (km/s)	2.5	~ 0	0
r_L (cm)	22.5	0.9	0.9
r_s (cm)	20	0.8	0.88
l_s (cm)	80	22	3.5
B_{ext} (T)	0.16	100	410
T_e+T_i (keV)	0.06	5	15
n (m^{-3})	1.1×10^{21}	2.5×10^{24}	1.4×10^{25}
E_p (kJ)	2.2	180	560
E (Pa)	1.5×10^{4}	6×10^{9}	10^{11}
τ_N (μs)	600	175	270

Figure 7: Anticipated FRC parameters from the validation experiment from merging, followed by a purely radial, and a purely axial compression. In the actual experiment the FRC radial and axial compressions would occur simultaneously.

edge magnetic field of 410 T (see Figure 7), with a compressed FRC length of 35 mm. From Eq. (5) a fusion gain G = 1.5 would result. If realized, this would be a remarkable achievement for such a modest experiment and would act as a testament to the cost and efficiency advantages of this approach to fusion.

The total gain desired from the IDLC is determined by the energy requirements to vaporize, ionize and energize the metal liner propellant to achieve a suitably robust plasma expansion or directed momentum for the space application. It is useful then to rewrite Eq. (5) in terms of the fusion energy produced per unit liner mass:

$$\frac{E_{fus}}{M_L} = G\left(\frac{E_L}{M_L}\right) = 4.3\times 10^{-8}\, M_L^{15/8}\, v_L^{4.75} \tag{7}$$

where Eq. (3) was used to put the expression in terms of the explicit liner variables. It can be seen that increasing either the liner mass, or velocity will increase the energy input into each liner particle.

3.1.2 Evaluation criteria for the metal liner

There is however a velocity limit for a given liner thickness. This set by a material's properties (electrical conductivity, melting point, and heat capacity) in order to avoid vaporization due to the inductive heating that the liner experiences during magnetic acceleration of the liner. As was first pointed out by Cnare in his landmark foil compression experiments, the liner's minimum thickness (mass) for a given liner velocity can be characterized by a parameter g_M defined by the "current integral":

$$\int_0^{t_m} I^2 dt = g_M A^2 \tag{8}$$

where I is the current flowing through the material cross-sectional area, A = w×δ, and where w is the hoop width and δ the hoop thickness. The driving force is simply the magnetic pressure ($B^2/2\mu_0$) applied over the surface area of the metal shell facing the coil when in close proximity to the driving coil. The current can be related to the force through Ampere's law which can be reasonably approximated as $B = \mu_0 I/w$. Normalizing to the action constant, g_{Al} for the vaporization of aluminum from an initial 300 °K, one finds for the maximum velocity for a given shell thickness δ:

$$v_{max} = 6.8x10^{10}\,\frac{g_M}{g_{Al}}\,\frac{\delta}{\rho_M} \tag{9}$$

where ρ_M is the shell material density. This should not be a significant issue during field compression due to the formation of a thick blanket at convergence. The initial thickness will typically be much greater than needed for the characteristic velocities (2-4 km/s) anticipated.

There are potentially several metals that could be employed. Not surprisingly, aluminum is a strong contender due to its low density and high conductivity, but lithium is not far behind. Possessing a low yield strength, a lithium liner would be especially advantageous in that the

initial thin shell could be readily extruded for positioning under the driver coils between pulses. For a given liner energy, its low mass density allows for thicker initial liner as well as a larger final shell radius. The latter is important for slowing down the fusion neutrons and extracting the maximum energy from the fusion products. Lithium also has several advantages as a plasma propellant. Recall that the ultimate fate of the shell is vaporization and ionization after intense fusion, Ohmic and radiative heating. For the space propulsion application lithium is to be favored for its low ionization energy thereby minimizing the frozen flow losses. Due to its low atomic mass it will also attain the highest exhaust velocity for a given fusion energy yield. For these reasons, lithium is the material of choice for the IDLC. From Eq. (9) one finds for lithium: v_{max} (km/s) = 16·δ(mm). The anticipated lithium liner thickness is several mm so there is no real issue here as high gain can be accomplished with liner velocities of 3-4 km/s. For the validation experiment aluminum is the clear choice due to its wide availability, low cost, and ease in handling.

3.1.3 Validation Experiment

The basic approach will be to test liner convergence with aluminum liners using the G-10 vacuum chamber and driver coil pair used for the Foil Liner Compression experimental testing at MSNW, but powered by the full energy storage and delivery system at the UW Plasma Dynamics Laboratory. The principle diagnostics to determine liner position as a function of time will be internal magnetic probes on axis, and axial arrays of external flux and B loops. End-on imaging of the liners will be obtained with a backlit fast framing camera. As in other liner experiments, both at MSNW and elsewhere[12,13] these images yield detailed information regarding liner uniformity during convergence. The liners will be constructed out of 6 cm wide, 0.2 mm thick aluminum strip and joined using an ultrasonic welding technique that maintains the structural, thermal and resistive properties of the material. After obtaining the proper convergence, the FLC chamber will be modified and equipped with the existing IPA FRC formation sections as depicted in Figure 8.

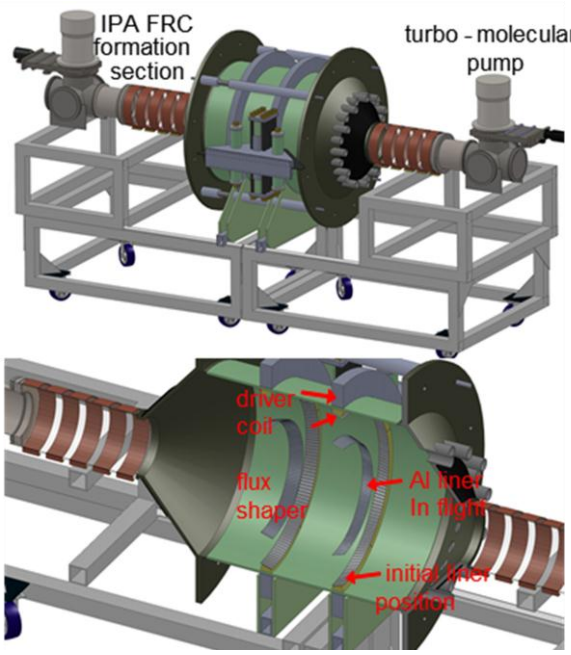

Figure 8: Foil Liner Compression testbed modified for validation experiments.

Detailed 2D, resistive Magneto-Hydrodynamic (MHD) calculations have been carried out to study the FRC formation and merging in this geometry, first with three and then two converging liner bands. It appears that for the *in situ* case (no overall translation of the liners as in

Figure 4), that two should be sufficient to assure proper axial and radial compression of the FRC. Internal rings can be employed if necessary. The result from a 2D MHD calculation of FRC merging with three rings is shown in Figure 9. The primary diagnostic of plasma compression and heating will be the neutron count from the D-D fusion reaction. The yield is a

sensitive measure of ion temperature. The signal will be analyzed using MCNP codes used in previous FRC experiments.[14] A soft x-ray camera will be used for plasma imaging and electron temperature measurements. Plasma density will be obtained from a cross-chamber HeNe laser-based interferometer.

The successful development of the 3D liner compression of the FRC will validate liner compression as a practical approach to achieving a small scale, low yield source of fusion energy. This method will facilitate the exploration and development of a new regime of fusion

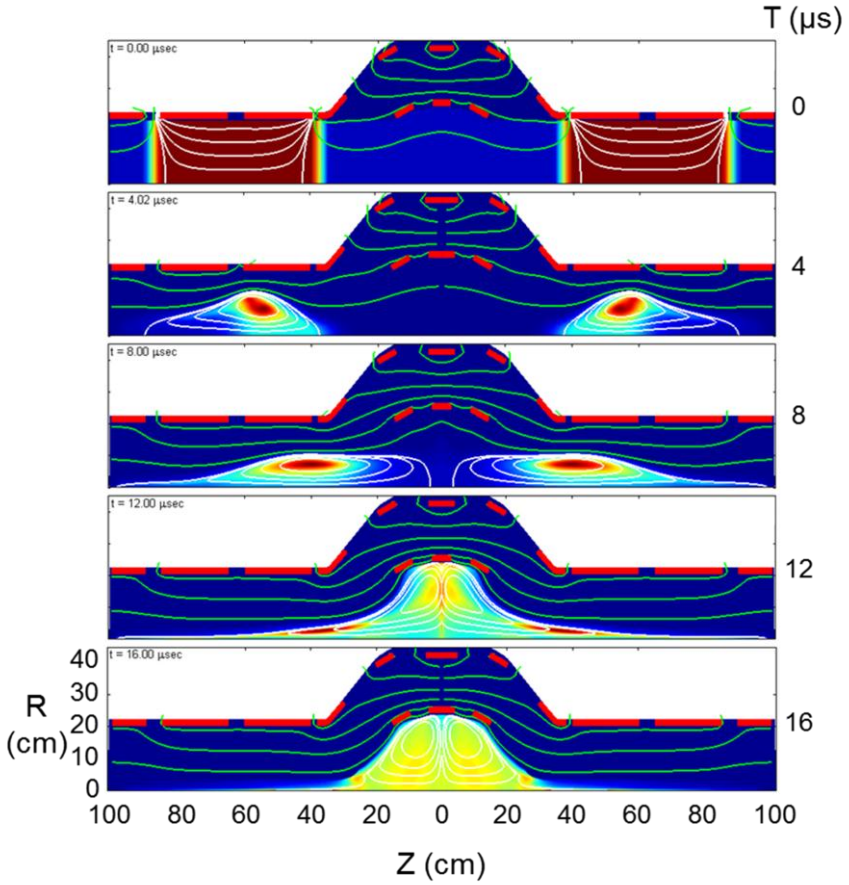

Figure 9: Pressure contours and flux lines from 2D MHD calculation of the formation and merging of FRCs inside three converging liners.

plasma physics that could lead to very different application and usage to that now being pursued by virtually all other fusion efforts. At a gain ~ 1-5 there would be application to the breeding of fissile fuel, particularly for the Thorium cycle, to support the future generation of advanced fission plants. There would also be application to the burning and transmuting of long-lived fission products and actinides from commercial fission.

The use of such the IDLC system for space propulsion is now being investigated at MSNW with a grant from NASA. The project represents a unique opportunity to gain the interest of a community that has the resources to rapidly develop the science and technology if the concept can be validated.

For the more ambitious goals of a high efficiency fusion power plant employing direct conversion or a fusion driven rocket, higher fusion gains (10 – 30) are desired. To achieve ignition, a fusion gain G > 5, along with sufficient magnetic field for the magnetic confinement of the fusion product alpha (^{4}He) within the FRC plasmoid will be needed. With fusion alpha heating, ignition conditions are achieved and the effective gain can be significantly increased, potentially to as large as several hundred. The necessary magnetic confinement is readily achieved in the compressed FRC plasmoid for the baseline parameters anticipated for the IDLC. While the scale of the validation test is set by the available equipment and energy storage at PDL, better standoff would be achieved by increasing the radius of coil driver for the full scale reactor. Increasing the driver radius by a factor of 2.5 (i.e. a one meter radius liner), the liner mass would also increase by this factor if one were to maintain the same liner velocity and width. This would be sufficient to increase the fusion gain to 6. To achieve a nominal fusion gain of 20, the liner velocity would need to be increased from 2.5 to 4 km/s. With the longer "stroke length" from a larger driver coil, should make this considerably easier to achieve.

3.2 Mission Definition

There is an inherent dependence between payload mass fraction, specific impulse, power, and trip time. For example a high payload mass fraction can be achieve with a higher Isp for a given payload at a fixed power but will require a longer trip time. These interdependencies have a strong bearing on mission design and were therefore chosen as the key parameters to investigate. Payload mass fraction was an obvious parameter to optimize in early mission studies. Defined here as the amount of payload delivered to the target destination over the total initial mass, it is one of the largest drivers of cost and feasibility of any future space mission. Current mass fraction are about 20% to LEO, 5% to Mars orbit, and 25% to Mars Surface, means that one quarter of one percent of a launch vehicle on Earth's surface will make it to the surface of Mars. This also means that at a cost of almost $1 million/kg the Martian surface remains a difficult hurdle. One of the largest ways to improve this is to increase the payload mass fraction for the Mars transfer. As will be shown in the analysis below payload mass fraction of 65% are feasible with The Fusion Driven Rocket.

Specific impulse is a parameter that is determined by the fusion condition of FDR, as will be discusses further in Section 3.2.1. The power is based on the require input energy into the fusion reaction to achieve the desired Isp and a realistic scaling of solar panels. The use of solar panel for fusion and their scaling will also be discussed further in this report. Finally, trip times are an important parameter for a multitude of reasons. Mission times factor into cost, public interest, mission success, and astronauts safety. For all this factors, faster is almost always better, however faster mission require much larger delta V. While a simple Hohmann transfer to Mars takes around 200 days, the delta V is only about 5 km/s. For the fusion driven rocket, where 30 day transfers were investigated, delta V reached as high as 45 km/s. Trade off studies between mission time, FDR burn time, and Delta V were conducted and are presenting in the following section.

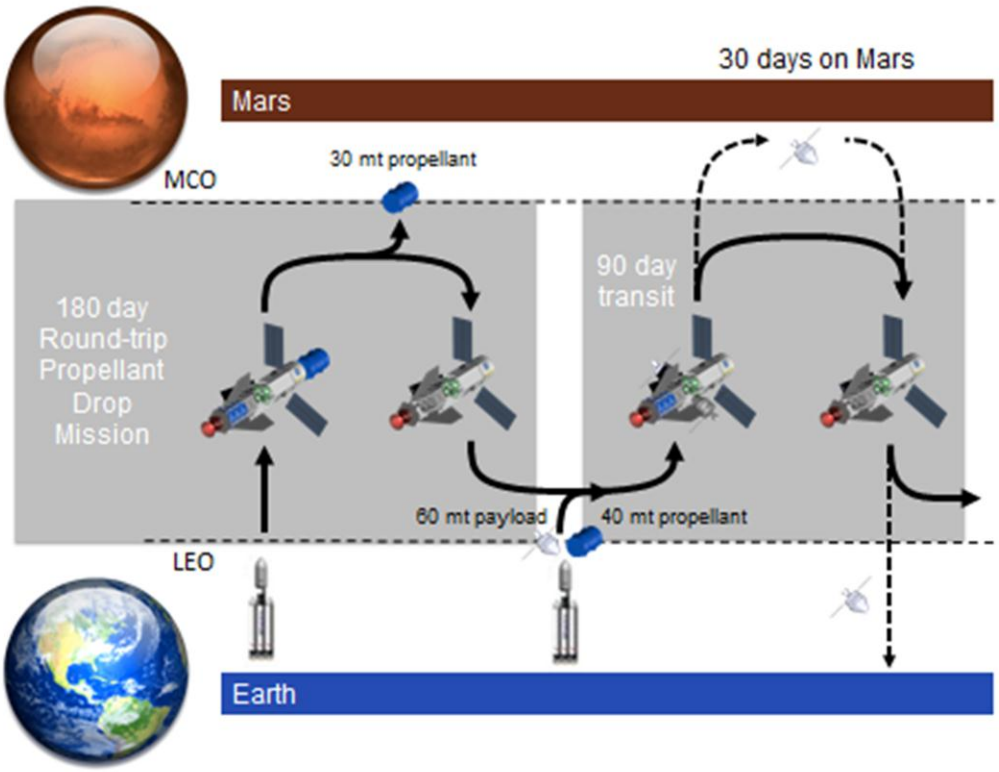

Figure 10: Sample manned mars mission architecture based on a fuel pre-deployment approach

Figure 10 illustrates a sample redeployed manned mars mission. In this mission architecture a single preliminary cargo mission is sent to Mars using the FDR spacecraft in almost the exact configuration that will be used in the second manned portion of the architecture. By keeping the transfer times same for all aspects of the mission, decreases operation variation and allow the spacecraft to be full flight qualified in the exact operating condition before it is ever manned. However it would certainly be appropriate to extend transfer times of the cargo mission in order to increase payload mass fraction as this phase of the architecture is often not as time sensitive. The purpose of the cargo mission will be to deploy a fuel store of lithium in a Martian orbit. The fuel will be required for the return portion of the manned mission. Estimates of the required propellant for the return trip allow flexibility of mission designers; giving the option for either more mass for mars exploration equipment or a small initial launch mass. As will be shown in the following section, launches required for the FDR Mars mission architecture are planned using HLV requiring no more than 130 mt to LEO. A single launch will be requiring for the pre-deployed cargo mission and a second for the manned mission. The FDR spacecraft will remain permanently in space after the initial launch and only fuel and payload will be required to rendezvous with the spacecraft for future trips to Mars.

3.2.1 Model of FDR and Mission Assumptions

An analytical model, based on a mission driven approach, was used to examine a direct Mars Transit utilizing a Fusion Drive Rocket (FDR). This was similar to the methodology employed

by NASA's Copernicus software to determine accurate mission profile and ΔV requirements as a function of mission transfer time and thruster burn time. Analysis was focused on a 90-day transit time to Mars. It was felt that this timescale was an appropriate balance between fast transfer time, required to protect astronauts from harmful space radiation, while still providing high payload mass fraction and low initial launch masses. Moreover, a 90-day trip can easily be accomplished with a conservative estimate of fusion gains that will be discussed in detail later. While faster trip times are possible, they come of course at the cost of decreased payload mass fraction. These numbers can be greatly improved by simply attaining large fusion gain with a consequent higher Isp from the FDR. However it was the intent of this work to focus on how, even with conservative estimates of fusion yield, FDR could revolutionize interplanetary space travel.

In addition to the primary 90-day mission, more ambitious mission profiles such as a 30-day Mars transit were examined in particular with regard to increased fusion ignition yields. While these higher gains are quite feasible they are not certain at this time, and therefore were not assumed for the first implementation studies of FDR, but rather analyzed to illustrate, once the physics of the FDR has a sound footing in both experiment and theory, what the potential of this technology could provide to manned space exploration.

The most relevant metric of the Fusion Driven Rocket is the energy gain of the fusion reaction. Thus the mission analysis included a trade study of various fusion gains. The primary fusion gain can be stated as a function of the liner mass, M_L, and the terminal velocity, V_L, (i.e. liner energy) at which the liner converges.

$$G_F = M_L^{1/2} G_I C E_{in}^{11/8} \tag{10}$$

Where G_I is the ignition gain, C is a fusion constant[15] equal to 4.3×10^{-8} and E_{in} is the energy input into the fusion reaction and is described by,

$$E_{in} = \frac{1}{2} M_L V_L^2 \tag{11}$$

For this analysis, the liner velocity was conservatively assumed to be no greater than 4 km/s. This is based on what has been demonstrated by previous experimental efforts, and is sufficiently less than the predicted vaporization limit of lithium due to inductive heating during liner acceleration.[16] A lower limit to the liner mass is found from the desire to have the liner thickness sufficient to have fusion neutron energy deposited in the liner [i.e. $r_L(\text{min}) \geq 5$ cm]. A mass of 0.37 kg was assumed for the total lithium liner mass which is well above the minimum amount of material (0.28 kg) needed.

In addition to this fusion gain, there is a likely possibility of an ignition gain due to additional heating of the plasma from the magnetically confined fusion product alpha (^{4}He) ions. The additional energy from fusion heated fuel varies significantly depending on assumptions of the liner dynamical behavior as well as the fusion burn propagation. The actual total gain that will be achieved is thus a complex hydrodynamic/materials physics question that will need to be addressed through further research. The codes for this calculation with modifications for a magnetized target are currently under development. The initial numerical calculations by Parks et al[17] indicate significant fusion ignition gains can be achieved even with only partial

thermalization of the fusion alphas. While this secondary ignition gain of the FDR is unknown, it is likely to be at least 2. Therefore, for the mission analysis presented here, ignition gain enhancements of 1 (no ignition gain) and 10 are examined along with the nominal gain of 2. The 1 and 10 cases are meant to bound the likely yield. With the liner mass and velocity having been determined, the primary fusion gain is determined from Eq. (10) with a fusion gain of 20.
With the total fusion gain assumed, the energy from the fusion reaction, E_{out}, can simply be determined as the gain multiplier times the energy input, E_{in}, into the reaction.

$$E_{out} = G_F E_{in} \tag{12}$$

The amount of energy from the fusion reaction that is actually converted into kinetic or propulsive energy is decreased by a thrust efficiency factor, η_T, and the major loss mechanism - the ionization of the lithium liner. This is described by the equation,

$$E_{kinetic} = \eta_T E_{out} - \phi_{ion} M_L \tag{13}$$

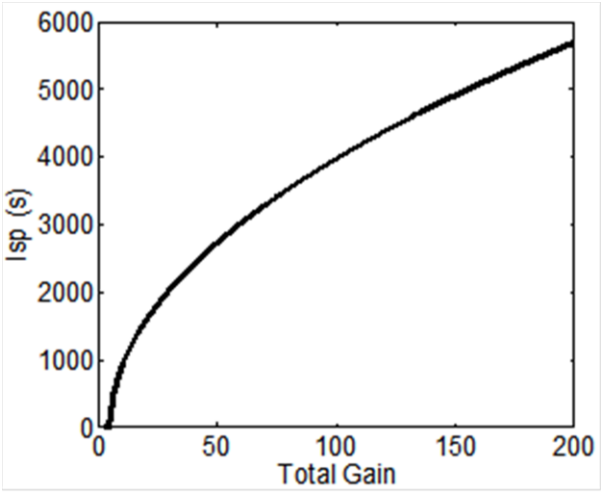

Figure 11: Projected Isp accounting for frozen flow losses as a function of total fusion gain.

Specific impulse can be determined as a function of the total gain (= fusion gain × a variable ignition multiplier) as shown in Figure 11 and described by the following equation,

$$I_{isp} = \frac{\sqrt{2E_k / M_L}}{g_0} \tag{14}$$

The resulting minimum expected I_{sp} for FDR is therefore 2,440 s, and could range as high as 5,720 s. Notice that the I_{sp} drops quickly at lower fusion gains. This is due to the rising significance of the lithium liner's ionization cost.

For a given mission architecture and desired transfer time a corresponding ΔV can be determined, as will be discussed in Section IV. By knowing the exhaust products of the fusion reaction determined above and this ΔV requirement, the mass ratio, *MR*, is set by the simple rocket equation,

$$MR = e^{\frac{\Delta V}{I_{sp} g_0}} \tag{15}$$

MR can also be defined as the initial mass of the spacecraft, M_i, over the final mass, M_f, of the spacecraft as represented in Eq. (16). Here, the final mass is just the mass of the payload, M_{PL}, plus the structural mass, M_S, of the spacecraft represented in Eq. (17). The initial mass is the same plus the mass of the propellant, M_P, need to carry out the mission, shown in Eq. (18). This propellant mass represented in Eq. (19) is simply the mass of the liner from the fusion analysis

times the frequency of operation, f, times the length of the mission, ΔT. The Mass of the Structure is broken down in Eq. (20). It is a function of the solar panel mass, capacitor mass need for the fusion propulsion system, and some addition mass, which has been chosen here to be 10% of the payload. The mass of the fusion system is defined as energy input into the fusion reaction divided by the specific mass of the capacitors, α_{cap}, required to supply that energy, and the mass of the solar panels is defined as the power required to charge the fusion caps divided by the solar panel specific mass, α_{SEP}. Finally the actually power need to run the fusion reactor is simple the energy input divided by the frequency of operation as written in Eq. (21).

$$MR = \frac{M_i}{M_f} \tag{16}$$

$$M_f = M_{PL} + M_s \tag{17}$$

$$M_i = M_{PL} + M_s + M_P \tag{18}$$

$$M_P = M_L f \Delta T \tag{19}$$

$$M_S = \frac{E_{in}}{\alpha_{cap}} + \frac{P_{SEP}}{\alpha_{SEP}} + 0.1 M_{PL} \tag{20}$$

$$E_{in} = \frac{P_{SEP}}{f} \tag{21}$$

Equations 16 through 21 represent a system of six equation and six unknowns: M_i, M_f, M_S, M_P, f, and P_{SEP}. Solving these equations simultaneously allows each to be determined and for an analytical feasibility study of FDR for a direct Mars transfer to be carried out.

There are several important assumptions made in the analytical analysis worth outlining here. The mass of the payload was chosen to be 61 MT, based on previous manned Mars mission analysis.[18,19] It was estimated that the coupling coefficient, or the amount of energy that is transferred from the capacitor to the fusion liner, is roughly 50%. It is important to note that the other 50% is not lost energy, but is returned to the capacitors from the driver coils as a normal aspect of the electrical circuit behavior. Therefore a higher or lower coupling efficiency only acts to increase or decrease the size of the energy storage, but not the power required. The liner itself is assumed to be 50% ionized from the fusion reaction and plasma products. The ionization energy loss, as with all plasma based thrusters, shows up as a frozen flow loss and can influence the performance FDR especially at low gain levels (lower Isp), as will be discussed later. The spacecraft for this analysis is assumed to consist of three main masses: (1) the propulsion system, (2) power system, and (3) propellant.

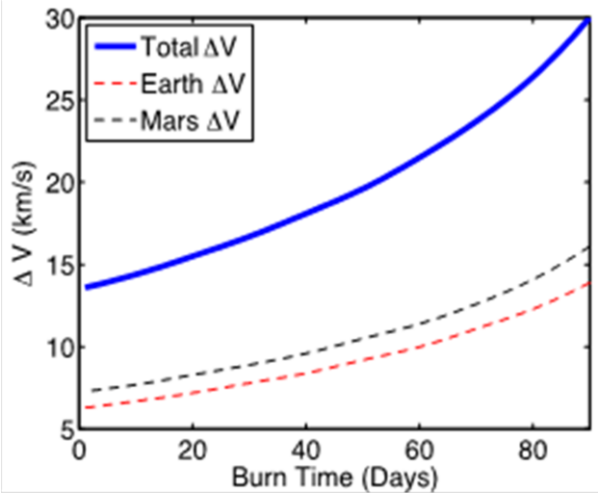

Figure 12: Projected Isp accounting for frozen flow losses as a function of total fusion gain.

The mass of the propulsion system is driven by the capacitor specific energy which is assumed to be ~ 1 kJ/kg. This number is conservative enough (one half of current state of the art hardware) to include the necessary cables and switches as part of this mass, as these masses will also scale with capacitor mass. The mass of the power system is based on a solar panel specific mass of 0.2 kW/kg. And finally, the mass of the propellant system is primarily tankage and assumed to be 10% of the lithium propellant mass. While the propellant is solid lithium and would not require significant tankage itself, the transfer, feed and liner formation equipment will be added mass. The last assumption worth noting is that this initial analysis assumed full propulsion capabilities for all orbital maneuvers, including the Mars insertion orbit. While other Mars mission architectures propose aerocapture, it was deemed not worth the propellant mass savings to increase risk and uncertainty inherent with aerocapture for this first order manned mission analysis.

As a reference mission a manned mission to Mars similar to that of the Design Reference Architecture (DRA) 5.0 [19] was chosen. In doing so, it was not difficult to show the potential of the Fusion Driven Rocket compared to nuclear thermal propulsion systems in terms of trip time, payload mass fraction, and initial launch masses. However, the implications of the FDR are even more far-reaching and warrant additional benefit analysis on pre-deployed missions. Furthermore, as a result of the high payload mass fraction associated with the FDR, single trip missions with no pre-deployed assets can be readily achieved. While this ultimately may require higher fusion gains, they are not outside of the anticipated limits of fusion yield.

3.2.2 Effects of Burn Time

With Isp determined, various mission parameters can be examined for a given ΔV. The lowest ΔV for a direct interplanetary transfer is the solution to the Lambert problem where short finite burns occur at the beginning and end of the transfer. While this is ideal from a mission perspective, it is not necessarily an optimum from a propulsion system point of view. As part of this study a 90-day Earth-Mars transfer was examined for a variety of infinite burn times using the FDR.

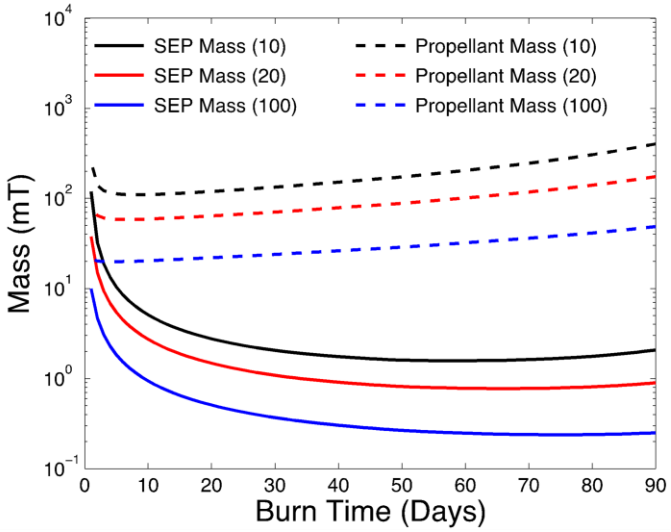

Figure 13: Mass of propellant and solar panel system as a function of burn time for a gain of 20, 40, and 100.

Figure 12 illustrates the ΔV requirements from a one-day to a continuous 90-day burn. It can be seen that the faster and stronger the burn, the less demanding the ΔV requirements as the value approaches that of the Lambert solution. However, even though the ΔV requirements are less, shortened burn time requires more energy in a shorter period of time, greatly increasing the power requirements. This trade-off between the mass of propulsion system and ΔV (mass of propellant) are the major mass drivers for the spacecraft and mission design. What is uniquely different here with the FDR is that the solar panel mass scales with the jet power (for fixed fusion gain) but the capacitor mass does not as the capacitors can be operated at higher or lower

rep rate to match power demand. The solar panel mass must increase if a higher power is desired in order to charge the capacitors at the higher rep rate. Figure 13 indicates the increase in propellant mass and decrease in solar panel mass as functions of burn time. These two mass functions create an optimal payload mass fraction for a given fusion gain, which can be seen for all possible gain cases within the design space as shown in Figure 14. For all fusion gains this optimal payload mass fraction occurs at around a 10-day burn time. For the expected gain of 40 this results in a payload mass fraction of 0.47. Ten days is also the optimum burn time when considering initial mass, resulting in a minimum initial mass of 130 MT, which is consistent with a single ETO launch.

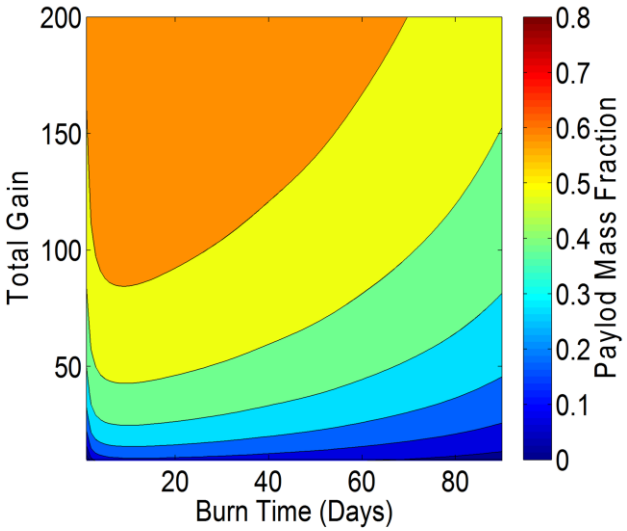

Figure 14: Payload mass fraction as a function of burn time and total gain

3.2.3 Effects of Solar Panel Size

From a mission perspective, solar panel size is determined from a desired payload mass fraction as shown in Figure 15. One of the most important conclusions illustrated by this figure is that payload mass fraction does not vary significantly near the optimal payload mass fraction. So while the optimal payload mass fraction of 47% at a gain of 40 requires a solar panel power of 546 kW, this could be lowered to 300 kW, with a marginal change in the payload mass fraction to 45%. Furthermore, the initial mass of the spacecraft is also not particularly sensitive to solar power near the optimal value, as can be seen in Figure 15. This is particularly true at higher gains. Ultimately, it will be necessary to determine the value of these trade-offs based on the desired characteristics of specific future Mars missions.

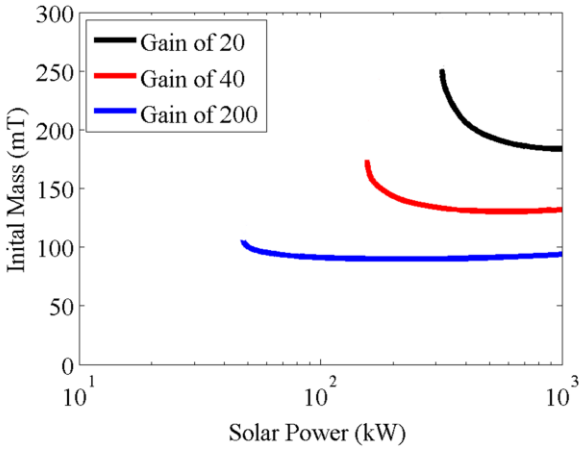

Figure 15: Initial mass as a function of required solar power for a gain of 20, 40, and 200.

In summary, Table 1 lists several important mission parameters for the complete range of fusion gain possibilities. It is clear that at an expected gain of 40 produces very favorable Isp, while keeping system mass and power requirements low for a 90-day transit to Mars. Even at an extremely low gain estimate of 20, the Fusion driven rocket still offers the best option for a manned mission to Mars, producing transit times and payload mass fractions that are not feasible with any other propulsion system

Table 1: Summary of the FDR parameters for a burn optimized 90 Mars transfer

Total Gain	20	40	200
Liner Mass (kg)	0.365	0.365	0.365
Isp (s)	1606	2435	5722
Mass fraction	0.33	0.47	0.68
Specific mass (kg/kW)	0.8	0.53	0.23
Mass Propellant (MT)	110	59	20
Mass Initial (MT)	184	130	90
SEP (kW)	1019	546	188

3.2.4 Effects of Advanced Mars Capture

As described in the DRA 5.0, advanced aerocapture was critical for manned Mars missions even assuming Nuclear Thermal Propulsion (NTP). Up to this point the analysis performed here has primarily focused on a manned transit to Mars without relying on aerocapture as this has usually been deemed too risky. Aerocapture is, however, favorable for cargo missions using NTP and if this type of mission maneuver is performed successfully and frequently, it may even become favorable for manned missions as well. Therefore, a preliminary investigation of aerocapture in conjunction with the Fusion Driven Rocket was investigated. To do so the same ΔV requirement for the trans-Mars insertion burn was conducted propulsively, with the Mars insertion burn being replaced by an aerocapture maneuver. The ΔV requirement for the propulsion system was therefore significantly less, thereby decreasing the amount of propellant needed. However, an additional mass of 40 MT was added to the spacecraft mass consistent with heat shielding as stated in the DRA 5.0. Due to the high Isp of the FDR, the amount of propellant is much less than both chemical and NTP propulsion systems. Only at a gain of 10, where the Isp is as low as 1,600 s, does the mass savings of propellant equal the mass of the heat shield. Therefore, it is evident that for all mission profiles and all possible fusion gains, there is no need to invoke aerocapture for mission feasibility. It is far more favorable and much lower risk to use the Fusion Driven Rocket for all orbital maneuvers.

3.2.5 30-Day transit to Mars

While a 90-day transit to Mars offers a good balance of payload mass fraction and transit time at even modest estimations of fusion gain, the possibility of very high energy yields make extremely rapid transits to Mars quite feasible. To investigate this, a 30-day transit to Mars was considered.

The ΔV budget for such a mission is very high, ranging from 98 km/s at a full 30 day burn to 45 km/s for a 0.1 Day-burn (which approximates the Lambert problem). For such high ΔV's a fusion again of 40 would not result in optimal mission parameters. More ambitious gains of 200, however, show that his mission is quite favorable. The optimal burn time for such a mission is 6 days, which results in a fairly high demand on solar power. As with the 90-day mission, a slightly off-optimal approach yields much lower solar panel mass without sacrificing much payload mass fraction or significantly increasing the initial spacecraft mass, as can be seen in Figure 16 and Figure **17**. With one MW solar electric power, a 30% payload mass fraction can be delivered to Mars in 30 days. For the 61 MT payload mass assumed for the 90-day mission, this results in an initial spacecraft mass of a reasonable 200 MT.

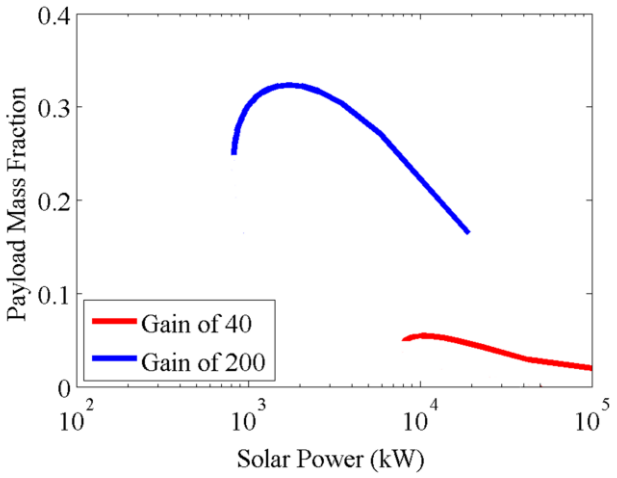

Figure 16: Payload mass fraction as a function of required solar power for a 30 day Mars transit for a total fusion gain of 40 and 200.

3.3 Spacecraft System Design

As part of the Phase I effort a preliminary spacecraft design was conducted to get an initial understanding of key component mass and overall spacecraft size. While a much more in depth and detailed analysis can and will be conducted under phase I, it was felt that even a small effort at this early stage would help give a better understanding of how revolutionary FDR can be compared to other more conventional interplanetary spacecraft systems. Based on the mission analysis conducted in Task 2 and presented in Section 3.2, a 90 day transit mission was chosen for the spacecraft design analysis. More specifically, the spacecraft design focused on the manned transfer vehicle. As illustrated, this mission architecture calls for a single spacecraft that acts as a transfer vehicle or an interplanetary tug between Earth and Mars. Therefore, while the spacecraft is scaled for a manned mission, the crewed habitat could easily be replaced with an equivalent payload mass.

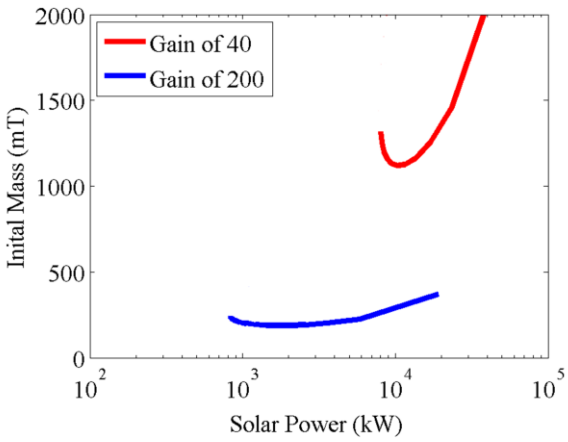

Figure 17: Initial Mass as a function of required solar power for a 30 day Mars transit for a total fusion gain of 40, and 200.

The 90 transfer vehicle is broken down into several large subsystem and categories. The Fusion Driven Rocket consists of 3 major components; (1) FRC formation, (2) Liner compression, and (3) Magnetic Nozzle. The majority of the mass of the fusion engine is

associated with the liner compression. This includes major items like energy storage and the magnetic coils themselves. Additional mass will also be required for power transition lines and high power switching. Also associated with the liner compression stage are the propellant tank and the propellant feed mechanism. Since the lithium propellant is a solid, the tankage required will be minimal. However, there is no clearly preferable liner insertion method at this time, so a generous mass budget was given to this particular subsystem. The thermal management that will be required for the FDR will be small for a propulsion system of this power level. This is primarily due to the large stand-off of the driver coils, and the fact that virtually all of the radiation and high energy particles will be absorbed by the liner/propellant and not the spacecraft. The liner driver chamber and magnetic nozzle will also intercept only a small fraction of the fusion neutrons escaping the liner as these structures allow for large apertures permitting the particles to escape into space with only minimal interaction with the spacecraft. The actual heat load from the fusion pulse will be the subject of MCNP analysis during phase II. At this stage in the design, the spacecraft structure is a miscellaneous category that is the sum of the minor spacecraft components not fitting into the other major systems. This includes, but is not limited to, support structure, shields and fairings, communication systems, data handling, attitude control systems, and batteries. Table 2 contains a summary of the mass of the fusion driven rocket for a 90 day transit to mars with a fusion gain of 40.

Table 2: Summary of spacecraft component masses

Spacecraft Component	Description	Mass (kg)
Spacecraft structure	Fairings, support structure, communication, data handling ACS, Batteries	7,300
Propellant tank	Lithium containment vessel	100
FRC Formation	Hardware responsible for formation and injection of Fusion material (FRC)	200
Propellant Feed	Mechanism responsible for formation and insertion of propellant liner	1,200
Energy storage	Capacitors	800
Liner driver coils	Electromagnetic coil used to drive inductive liner	600
Switches and cables	Pulsed power electronic components need to charge and discharge capacitor bank	300
Solar Panels	Solar panel array needed to supply power to propulsion system	2,700
Thermal Management	Radiator to coil fusion components	1,300
Nozzle	Magnetic nozzle used to protest spacecraft structure and direct fusion products	500
Spacecraft Mass		**15,000**
Crew habitat	Crewed compartment, atmospheric conditioners, oxygen, food water,	61,000
Propellant	Lithium	59,000
Total Mass		**135,000**

Figure 18 shows a conceptual rendition of the Fusion Driven Rocket Spacecraft. All the major components have been scaled appropriately. Most notably the Fusion Driven Rocket engine has a driver coil radius of 1 m. The rest of the spacecraft is scaled to be less than 9m in diameter to fit within the future Space Launch System (SLS) design. The radiators and the solar panels are both deployable so that they can either face away or towards the sun for maximum effectiveness. The solar panels where scaled to provide the 300 kW of power need to run the fusion reaction at the appropriate rep rate. The propellant volume is based off the density of solid lithium. Oxygen tank, crew habitat and payload have allow been added. For additional reference, the payloads shown here are Apollo Command/Service modules (CSM) which have a height of 11 m and a diameter of 4 m and weigh about 30 mt each

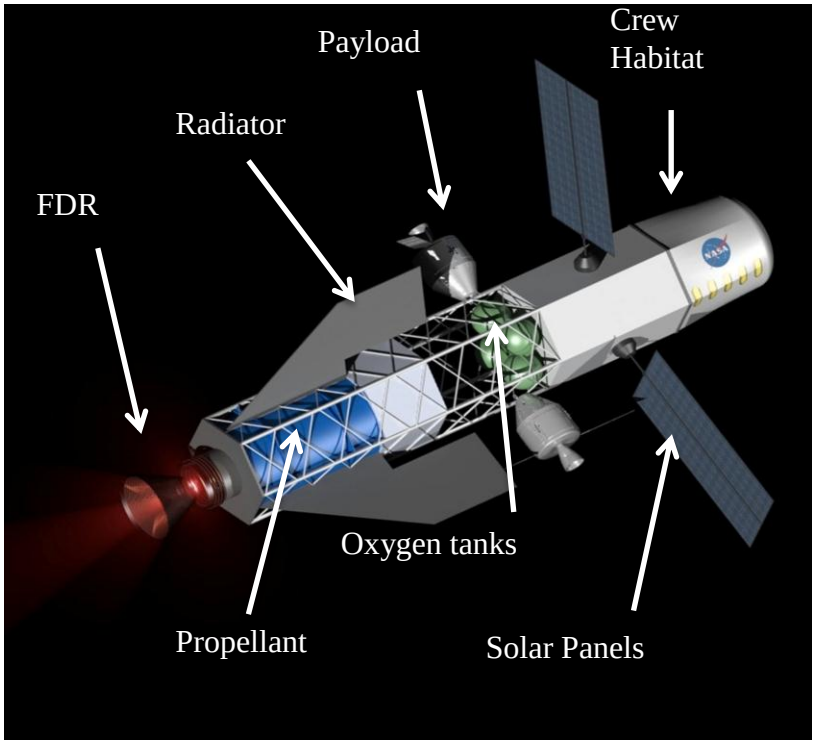

Figure 18: Conceptual image of the FDR spacecraft

4. Future Development and Path Forward

One of the key objectives of Phase I was to formulate a path forward for the Fusion Driven Rocket. FDR offers a major change for the future of interplanetary travel. It was felt that it was important to determine the key technological milestones and the time frame for their completion. The technological roadmap for the FDR can be found in Figure 19. Several technologies, such as the Solar Power and Energy Storage, are already of a flight qualified level. The Charging, Shielding, and Thermal systems are all of a moderate TRL as these would mainly be adaptations of those currently employed in fully developed space systems.

The overall FDR system ranges from relative high TRL components (such as the FRC formation system) down to very low TRL components (such as the fusion compression chamber). The lower TRL components have been the focus of the NIAC phase I effort and will be developed to higher TRL throughout the phase II of this project. A Concept Validation Experiment will be conducted during the phase II effort with the possibility of demonstrating fusion gain if successful. It is expected at this point that NASA will have a strong interest in fully developing this system, and integrating it into their future space flight planning. With adequate resources a subscale ground demonstration could be realized as soon as 2017 and an in-space demonstration mission as early as 2023.

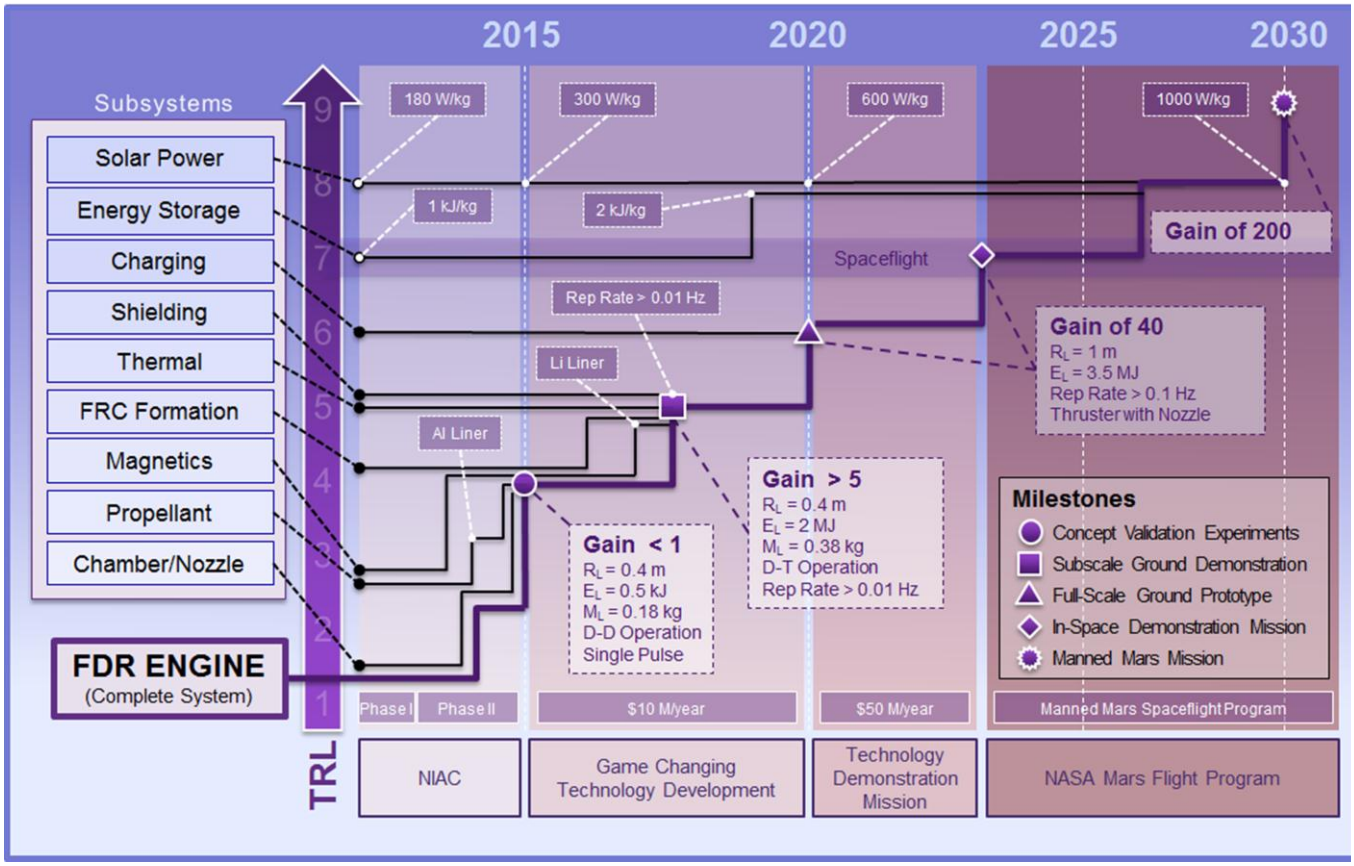

Figure 19: FDR Technology Roadmap

6. Personnel

6.1 Key Contractor Participants/Roles

Dr. John T Slough - Principle Investigator
Dr. Anthony Pancotti - Mission Analysis and Spacecraft Design Lead
Dr. David Kirtley - Mission Analysis and Structural Analysis
Mr. Michael Pfaff - Design and Drafting
Mr. Christopher Pihl - Spacecraft Design and Pulse Power

6.2 Key NASA Participants

John M. Falker, HQ - NIAC Program Executive
Jason E. Derleth, HQ - Senior Technology Analyst
Jerry Condon, NASA Johnson Space Center - COPERNICUS code support
Douglas A Craig - Mission Design Guidance and Advice

References

[1] Borowski, S. K., et al, "*Nuclear Thermal Rockets: Key to Moon - Mars Exploration*," Aerospace America, Vol. 30, No. 7, July 1992, pp. 34-37.

[2] Williams, C.H., Borowski, S.K., Dudzinski, L.A., and Juhasz, A.J., *"A Spherical Torus Nuclear Fusion Reactor Space Propulsion Vehicle Concept for Fast Interplanetary Piloted and Robotic Missions"*, 35th AIAA/ASME/SAE/ASEE Joint Propulsion Conference, AIAA 99-2704, June 1999.

[3] Drake, R.P., Hammer, J.H., Hartman, C.W., Perkins, L.J., and Ryutov, D.D., *"Submegajoule liner implosion of a closed field line configuration"* Fusion Technology, Vol. 30, pg. 310 (1996)

[4] M.M. Basko, A.J. Kemp, J. Meyer-ter-Vehn, *"Ignition conditions for magnetized target fusion in cylindrical geometry"***,** Nuclear Fusion, **40**, 59 (2000).

[5] Cnare, E.C., *"Magnetic Flux Compression by Magnetically Imploded Metallic Foils"*, Journal of Applied Physics, Vol. 27, No. 10, pg. 3812, (1967)

[6] Y. H. Matsuda, F. Herlach, S. Ikeda, and N. Miura, *"Generation of 600 T by electromagnetic flux compression with improved implosion symmetry"***,** Rev. Sci. Instrum**. 73** 4288 (2002).

[7] Slough J., et al., "*Confinement and Stability of Plasmas in a Field Reversed Configuration",* Phys. Rev. Lett., Vol. 9, 2212 (1992)

[8] G. Votroubek and J. Slough, *"The Plasma Liner Compression Experiment"*, Journal of Fusion Energy **29**, 571 (2010)

[9] Slough J.T., et al "*Transport, energy balance, and stability of a large field-reversed configuration"*, Physics of Plasmas **2,** 2286 (1995)

[10] A.A. Harms, K.F. Schoepf, G.H. Miley, D.R. Kingdom, 2002 *Principles of Fusion Energy*, World Scientific Publishing, Singapore 912805, pgs. 267-277.

[11] J. H. DEGNAN, ET AL. "Compression of Plasma to Megabar Range using Imploding Liner". *Phys. Rev. Lett.*, **82,** 2681(1999).

[12] E.C. CNARE, "Magnetic Flux Compression by Magnetically Imploded Metallic Foils", *Journal of Applied Physics*, Vol. 27, No. 10, pg. 3812, (1967).

[13] J. SLOUGH, ET AL., "Confinement and Stability of Plasmas in a Field Reversed Configuration", *Phys. Rev. Lett.*, **79**, 2212 (1992).

[14] G. VOTROUBEK and J. SLOUGH, "The Plasma Liner Compression Experiment", *J. of Fusion Energy* **29**, 571 (2010).

[15] Slough, J., Kirtley, D., Pancotti, A., Pfaff, Pihl, C., Voltroubek, G., "A Magneto-Intertial Fusion Drivem Rocket", ICOPS 1P-125 (2012)

[16] Kirtley, D., Slough, J., Schonig, J., Ketsdever, A., "Pulsed Inductive Marcon Propulsion", JANNAF 2010

[17] D.D. Ryutov and P.B. Parks, "Reaching High-Yield Fusion with a Slow Plasma Liner Compressing a Magnetized Target", Fusion Science and Technology, (2008)

[18] Drake, Bret G., Reference Mission Version 3.0 Addendum to the Human Exploration of Mars: The Reference Mission of the NASA Mars Exploration Study Team, Lyndon B. Johnson Space Center, NASA/SP—6107–ADD, 1998

[19] Drake, Bret G., Mars Human Exploration Mission DRA 5.0, NASA-SP-2009-566, July 2009